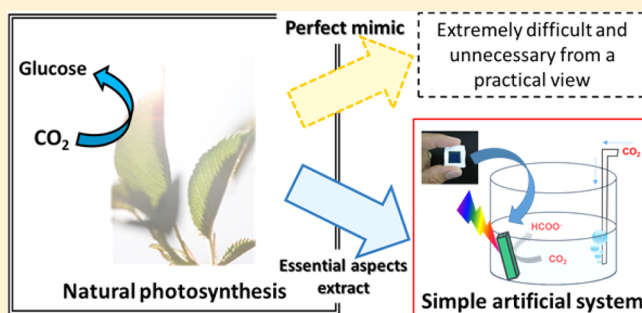


Toward Solar-Driven Photocatalytic CO₂ Reduction Using Water as an Electron DonorShunsuke Sato,^{*,†,‡} Takeo Arai,[†] and Takeshi Morikawa[†][†]Toyota Central Research and Development Laboratories, Inc., Nagakute, Aichi 480-1192, Japan[‡]PRESTO, Japan Science and Technology Agency, 4-1-8 Honcho, Kawaguchi-shi, Saitama 332-0012, Japan

S Supporting Information

ABSTRACT: Developing a system for the production of organic chemicals via CO₂ reduction is an important area of research that has the potential to address global warming and fossil fuel consumption. In addition, CO₂ reduction promotes carbon source recycling. Solar energy is the largest exploitable resource among renewable energy resources, providing more energy to Earth per hour than the total energy consumed by humans in 1 year. This report describes the advantages and disadvantages of the available CO₂ reduction and H₂O oxidation photocatalysts and the conjugation of photocatalytic CO₂ reduction with H₂O oxidation for the creation of an artificial photosynthesis system. In this system, CO₂ photoreduction and H₂O photooxidation proceeded simultaneously within one system under sunlight irradiation using a hybrid of semiconductors and molecular metal-complex catalysts.



1. INTRODUCTION

Developing a system for the synthesis of fuel or useful organic substances from carbon dioxide (CO₂) to help mitigate global warming and fossil fuel shortages is an active research area. In addition, CO₂ reduction promotes carbon source recycling. Reduction of CO₂ using water (H₂O) as both an electron donor and a proton source can be used to develop an artificial photosynthetic system for the conversion of H₂O and CO₂ into CO₂ reduction products such as carbon monoxide (CO), formate, methanol, and oxygen (O₂) using sunlight.

Most plants use an efficient CO₂ reduction system initiated by sunlight. Photosynthesis in plants involves solar-to-chemical energy conversion using an elaborate system of interconnected light-harvesting systems, highly efficient charge separation functions, and the reaction centers Photosystem I and II (PSI and PSII), followed by a dark reaction of the electron-transport chain of the cytochrome with coenzyme NADPH as a redox carrier and the Calvin cycle for CO₂ reduction. These key features and their mechanisms have been studied extensively, and a large number of reports and reviews on underlying photosynthesis processes have been reported.^{1–5} However, developing a mimic of the photosynthetic system is extremely difficult. Thus, a simple artificial photosynthesis system incorporating only the most essential aspects of photosynthesis (e.g., CO₂ reduction combined with H₂O oxidation using the Z-scheme system) can be useful. This report focuses on the development of an artificial photosynthesis system consisting of CO₂ photoreduction and H₂O photooxidation conjugated within one system operating under natural or simulated sunlight.

2. CONJUGATION OF PHOTOCATALYTIC CO₂ REDUCTION AND H₂O OXIDATION SIGNIFICANT FOR ARTIFICIAL PHOTOSYNTHESIS

2.1. Metal-Complex Photocatalysts for CO₂ Reduction and H₂O Oxidation. Photocatalysis using metal complexes has been reported for CO₂ reduction^{6–32} and H₂O oxidation.^{33–41} Quantum efficiency and product selectivity are high; e.g., the quantum yield of conversion of CO₂ to CO was as high as 0.82 with *fac*-[Re(bpy)(CO)₃MeCN]⁺ (bpy = 2,2'-bipyridine) using a rhenium ring oligomer as a photosensitizer and sacrificial electron donor.²⁸ A homogeneous catalyst based on a vanadate-centered polyoxometalate complex can act as a H₂O oxidation photocatalyst with [Ru(bpy)₃]²⁺ as a photosensitizer and persulfate as a sacrificial electron acceptor. The quantum efficiency of O₂ formation using this catalyst was approximately 0.68.⁴¹ These metal-complex catalysts possessed good photocatalytic ability for CO₂ reduction and H₂O oxidation. However, because of the different reaction conditions required for CO₂ reduction and H₂O oxidation, functionally conjugating CO₂ reduction with H₂O oxidation using metal-complex catalysts is difficult, as is inducing a continuous selective reaction in a mixture of reactants and products. The reoxidation of organic substances generated during CO₂ reduction and the rereduction of O₂ from H₂O

Special Issue: Small Molecule Activation: From Biological Principles to Energy Applications

Received: November 21, 2014

Published: February 13, 2015

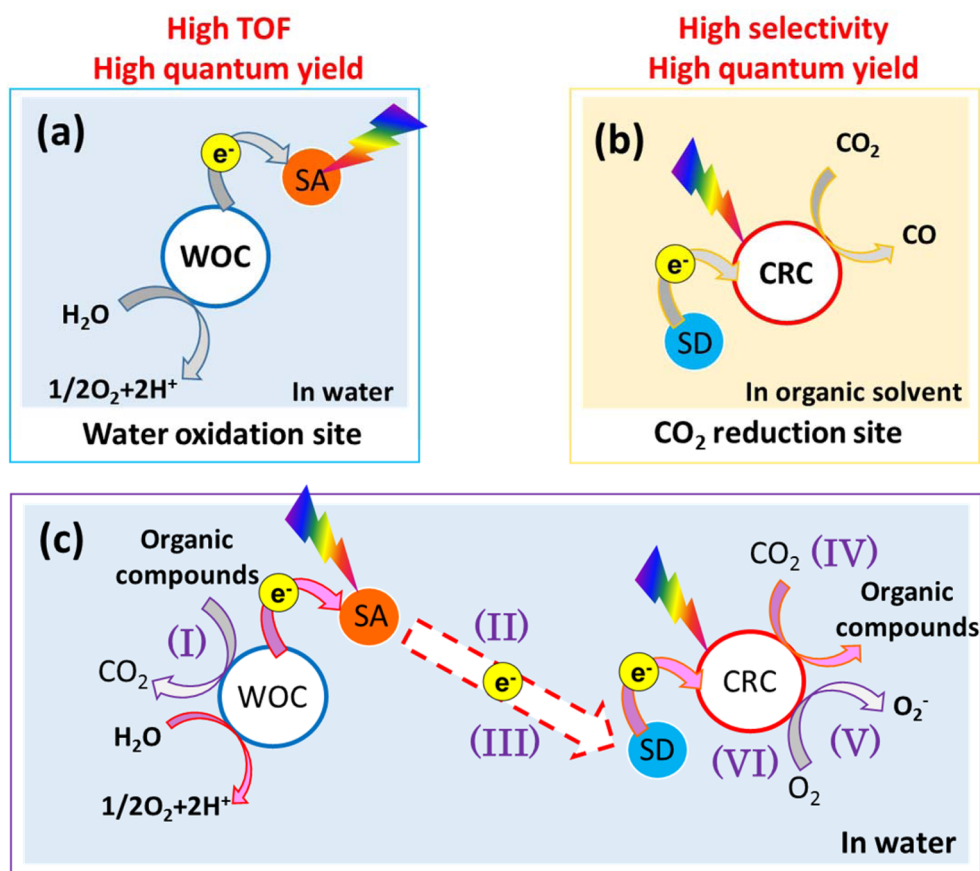


Figure 1. Advantages and disadvantages of metal-complex catalysts for H_2O oxidation and CO_2 reduction: (a) advantages of H_2O oxidation of a metal-complex catalyst (WOC) with a sacrificial electron acceptor (SA); (b) advantages of CO_2 reduction for a metal-complex catalyst (CRC) with a sacrificial electron donor (SD). (c) Problems combining WOC and CRC: (I) reoxidation of products such as organic compounds; (II) electron transfer from WOC to CRC; (III) need to be electron storage; (IV) need to be active in H_2O ; (V) easier reduction of O_2 than CO_2 ; (VI) stability in H_2O .

oxidation prevent the continuous reaction of H_2O oxidation and CO_2 reduction. These issues are summarized in Figure 1. Therefore, no study on photocatalytic CO_2 reduction conjugated with H_2O oxidation using only metal-complex catalysts has been reported. To construct a homogeneous system consisting of a metal complex for CO_2 reduction and H_2O oxidation, technical difficulties of a closed system, such as different reaction condition needs, inefficient electron transport between reduction and oxidation catalysts, short lifetimes of one-electron-reduced species, and short lifetime of the photoexcited state in the presence of O_2 generated by H_2O oxidation, must be overcome.

2.2. Semiconductor Photocatalysts for CO_2 Reduction and H_2O Oxidation. Semiconductor catalysts possess photocatalytic ability for the reduction of CO_2 ^{42–51} and the oxidation of H_2O .^{52–62} Many studies on CO_2 reduction conjugated with H_2O oxidation using semiconductor photocatalysts have been reported. Hydrocarbons were detected from residual carbon species on semiconductor surfaces.^{63,64} These results indicated that a possible experimental error (CO_2 reduction products from residual carbon species) may occur for photocatalytic CO_2 reduction using semiconductor catalysts when the amount of product is small compared to the amount of catalyst. However, isotope experiments have not confirmed that the photo-reduction products were converted from CO_2 molecules or that a stoichiometric reaction occurred in the production of O_2 from H_2O . In contrast, Ag-doped $\text{BaLa}_4\text{Ti}_4\text{O}_{15}$ photocatalyst acted as

a CO_2 reduction catalyst in aqueous solution under ultraviolet (UV)-light irradiation, with a ratio of $[\text{CO} + \text{hydrogen} (\text{H}_2)]/\text{O}_2$ of 2.0, indicating a stoichiometric reaction.⁴⁷ This indicated that H_2O was consumed as a reducing agent for the overall reaction to reduce CO_2 with the semiconductor. However, in this case, because of the large band gap of the semiconductor, the efficiency for solar energy conversion was very low. Regardless, the Ag-doped $\text{BaLa}_4\text{Ti}_4\text{O}_{15}$ system had the advantage of high selectivity for CO_2 , indicated by the ratio of CO/H_2 (about 2.0), which was high compared to that of other semiconductor systems. In contrast, CO_2 reduction for the production of fuels in aqueous solution using semiconductor photocatalysts is limited by the preferential H_2 production and low selectivity for the carbon species produced. These advantages and disadvantages are summarized in Figure 2. Semiconductors also have been studied extensively for H_2 production through H_2O splitting.^{65–73} However, the selectivity of the products for CO_2 reduction and the quantum efficiency in visible light must be improved. Furthermore, reoxidation of reduced carbon species along with complementary H_2O oxidation must be prevented when CO_2 reduction products remain in the liquid phase of the reactor.

2.3. Semiconductor/Metal-Complex Hybrid Photocatalyst for CO_2 Reduction. One advantage of metal-complex catalysts for CO_2 reduction is high efficiency,^{6–32} while one disadvantage is the unavailability of H_2O as an electron donor under the conditions of photocatalytic CO_2

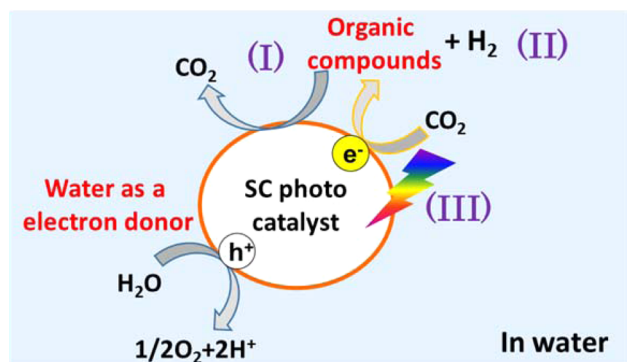


Figure 2. Advantages and disadvantages of a semiconductor (SC) photocatalyst for H_2O oxidation and CO_2 reduction. Disadvantages of a SC photocatalyst for CO_2 reduction: (I) reoxidation of products such as organic compounds; (II) low selectivity and quantum yield; (III) UV light.

reduction. In contrast, a semiconductor catalyst can use H_2O as an electron donor under the conditions used for photocatalytic CO_2 reduction.^{42–51} However, CO_2 reduction in aqueous solution is limited by low quantum efficiency due to preferential H_2 production under visible light. If semiconductors with high selectivity for CO_2 reduction could be developed for metal-complex catalysts, highly selective photocatalytic CO_2 reduction could be achieved, even in aqueous solution. This also could be applied to the Z-scheme system, which uses heterogeneous semiconductors with different band-energy potentials for CO_2 reduction and H_2O oxidation (Figure 3).^{69–73} Therefore, the

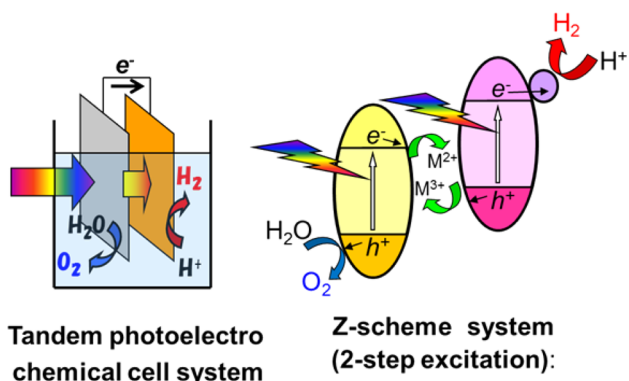
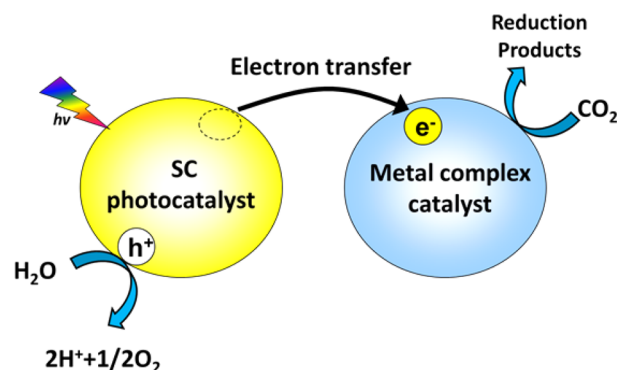


Figure 3. Schematic illustration of the total reaction of the Z-scheme system for H_2 production.

goal was to combine photoactive semiconductors with metal-complex catalysts capable of reducing CO_2 . The transfer of photoexcited electrons from the conduction band minimum (CBM) of the semiconductor to the metal-complex catalyst is essential to promote selective CO_2 reduction on the metal complex (Scheme 1). Only one report exists on the photocatalytic reduction of CO_2 by combining photoactive semiconductors and metal-complex catalysts.⁷⁴

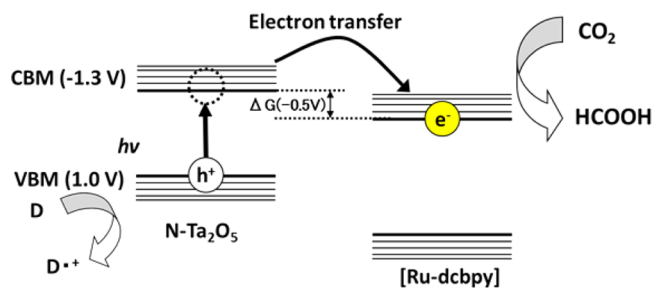
To prove the concept of a semiconductor/metal-complex hybrid photocatalyst for selective CO_2 reduction, metal-complex catalyst $[\text{Ru}(\text{dcbpy})_2(\text{CO})_2]\text{Cl}_2$ ($[\text{Ru}(\text{dcbpy})]$ (dcbpy = 4,4'-dicarboxy-2,2'-bipyridine) possessing electrocatalytic CO_2 reduction was used.^{75,76} The CO_2 reduction potential over $[\text{Ru}(\text{dcbpy})]$ was measured using cyclic voltammetry in acetonitrile (MeCN) saturated with CO_2 . The CO_2 reduction potential, which produced large peaks originating from

Scheme 1. Schematic Illustration of the Semiconductor/Metal-Complex Hybrid Photocatalyst



secondary electron injection into CO_2 molecules through $[\text{Ru}(\text{dcbpy})]$, was ca. -0.8 V (vs normal hydrogen electrode, NHE). Therefore, the potential of the CBM (E_{CBM}) of the semiconductor should be much more negative than the reduction potential for CO_2 over $[\text{Ru}(\text{dcbpy})]$ to facilitate electron transfer from a semiconductor in a photoexcited state.⁷⁷ For the present study, a NTa_2O_5 semiconductor powder with an orthorhombic Ta_2O_5 crystalline structure, which absorbs visible light at wavelengths shorter than 520 nm, was prepared.⁷⁸ Nitrogen doping not only causes a red shift of 200 nm at the absorption edge of Ta_2O_5 (Ta_2O_5 absorbs UV light <320 nm) as does N-doped TiO_2 ,⁷⁹ but it also provides p-type conductivity as in N-doped ZnO . The ionization potential, or the valence band maximum (VBM), of NTa_2O_5 was approximately $+1.1$ V (vs NHE), as determined by photoelectron spectroscopy in air.⁸⁰ The shift of the band potential of Ta_2O_5 to a more negative position upon nitrogen doping was favorable. The resulting E_{CBM} was calculated to be -1.3 V (vs NHE); therefore, the ΔG value (defined for the energy difference between E_{CBM} of a semiconductor and the CO_2 reduction potential in a molecular metal-complex catalyst) for E_{CBM} of NTa_2O_5 and the reduction potential of the ruthenium complexes was -0.5 V (Scheme 2). The hybrid photocatalyst

Scheme 2. Energy Diagram of the $\text{NTa}_2\text{O}_5/[\text{Ru}(\text{dcbpy})]$ Hybrid Photocatalyst for CO_2 Reduction



composed of NTa_2O_5 and $[\text{Ru}(\text{dcbpy})]$ ($\text{NTa}_2\text{O}_5/[\text{Ru}(\text{dcbpy})]$) promoted photocatalytic CO_2 reduction in an organic solvent under visible light; the main product was formic acid (HCOOH ; Figure 4). Only $[\text{Ru}(\text{bpy})]$ and NTa_2O_5 did not exhibit photocatalytic activity for CO_2 reduction, showing a turnover number (TN_{HCOOH}) per metal-complex catalyst of 89 using a sacrificial electron donor such as triethanolamine (TEOA) under visible light. The quantum yield measured for HCOOH formation was approximately 1.9% at 405 nm.

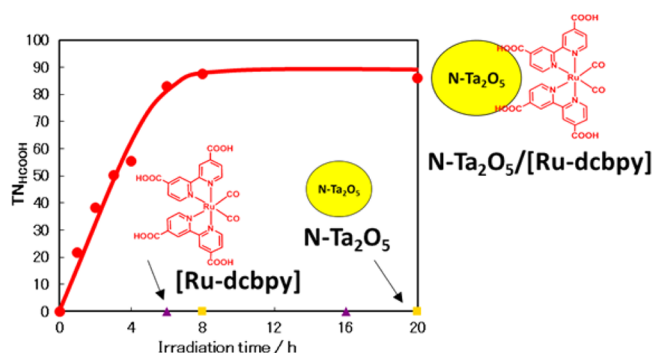


Figure 4. TN_{HCOOH} from CO_2 as a function of the irradiation time. Solutions were irradiated ($410\text{ nm} \leq \lambda \leq 750\text{ nm}$) using a xenon lamp. The concentrations of the photocatalysts were 0.05 mM and 5 mg for the ruthenium complexes and semiconductors, respectively, in a CO_2 -saturated 5:1 MeCN/TEOA solution. Catalysts used were [Ru-bpy] (purple triangles), NTa_2O_5 (orange squares), and $NTa_2O_5/[Ru-dcbpy]$ (red circles). Adapted with permission from ref 74. Copyright 2010 John Wiley & Sons, Inc.

A semiconductor/metal-complex hybrid catalyst can be applied broadly to many semiconductors and metal-complex catalysts. Therefore, the photoactivity, selectivity, and long-term stability could be enhanced by the choice of materials. Reports have indicated that the activity could be improved by changing the carboxylic anchor of bpy in the ruthenium complex to phosphate⁸¹ and that combinations with different photoactive semiconductors and metal-complex catalysts could promote visible-light-activated CO_2 reduction.^{82–86} The hybrid photocatalyst concept compensates for the disadvantage of metal-complex catalysts and semiconductor photocatalysts.

3. HYBRID PHOTOCATALYST FOR SOLAR-DRIVEN CO_2 REDUCTION UTILIZING H_2O AS AN ELECTRON DONOR

3.1. Semiconductor/Metal-Complex Hybrid Photocatalyst for CO_2 Photoreduction in Aqueous Solution. To reduce CO_2 using H_2O as an electron donor, CO_2 photoreduction must be conducted in aqueous solution. [Ru-dcbpy] is known to act as an efficient catalyst for CO_2 reduction even in aqueous solution. However, the first hybrid photocatalyst, $NTa_2O_5/[Ru-dcbpy]$, can operate only in an organic solvent because of the instability of the connection between NTa_2O_5 and [Ru-dcbpy]. Therefore, the concept of a hybrid photocatalyst was applied to a system functional in aqueous solution. A ruthenium complex polymer catalyst ($[Ru(L-L)(CO)_2]_n$, where L-L = a diimine ligand) reported by Deronzier et al.⁸⁷ and a p-type InP (zinc-doped indium phosphide wafer) were used in the hybrid system. The surface of an InP wafer was coated with a mixture of $[Ru\{4,4'\text{-di}(1H\text{-pyrrolyl-3-propylcarbonate})\text{-}2,2'\text{-bipyridine}\}(CO)(MeCN)Cl_2]$ (MCE1) and $[Ru(4,4'\text{-diphosphate ethyl-}2,2'\text{-bipyridine})-(CO)_2Cl_2]$ (MCE2-A) (Figure 5) using chemical polymerization. Transient optical spectroscopy revealed that accelerated electron transfer from the conduction band of the semiconductors in a photoexcited state to the complexes occurred via anchoring groups of the bpy ligand of the complexes linked to the surface of the semiconductors in the $CdSe/[Re(dcbpy)-(CO)_3Cl]$ system⁸⁸ and the $NTa_2O_5/[Ru(dcbpy)_2(CO)_2]^{2+}$ photocatalyst.⁷⁴ Because MCE2-A has 4,4'-diphosphate ethyl-2,2'-bipyridine anchor ligands, MCE2-A links tightly to the surface of InP.⁸⁹ A solar simulator equipped with an air mass

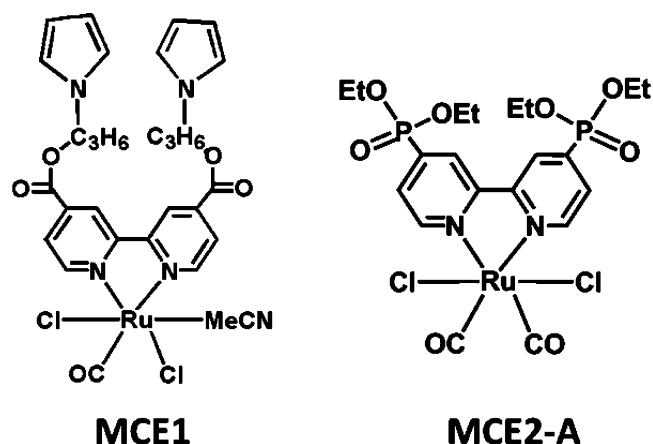


Figure 5. Structures of metal-complex catalysts.

1.5 filter (AM 1.5) with the intensity adjusted to 1 SUN (the intensity is 100 mW cm^{-2}) was used as a light source. Linear-sweep voltammograms of the InP electrode modified with a mixture of MCE1 and MCE2-A (InP/[MCE1+2-A]) were obtained in darkness or under simulated sunlight irradiation as CO_2 or argon gas was bubbled into the solution using a three-electrode configuration system (Figure 6). A clear CO_2

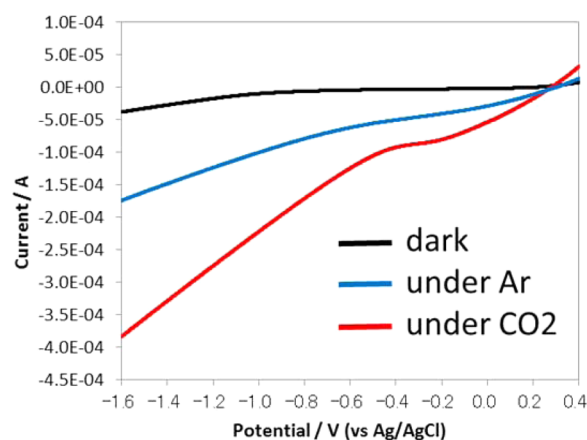


Figure 6. Linear-sweep voltammetry of an InP/[MCE1+2-A] photocatalyst in the dark (black line) or under simulated sunlight (1 SUN) in the presence of argon (blue) or CO_2 (red) gas.

reduction current was observed at $<0.0\text{ V}$ (vs Ag/AgCl) in aqueous solution under simulated sunlight. Figure 7 shows successive photoelectrochemical formate generation from CO_2 in pure H_2O over InP/[MCE1+2-A] using a three-electrode configuration under visible-light irradiation ($>422\text{ nm}$). The applied potential (-0.4 V vs Ag/AgCl) was set more positive than E_{CBM} of InP (-1.15 V vs Ag/AgCl), whereas no CO_2 reduction reaction occurred in darkness. InP/[MCE1+2-A] reduced CO_2 to formate under irradiation, while InP showed almost no activity for formate formation. Approximately $1.2\text{ }\mu\text{mol/h}\cdot\text{cm}^2$ of formate was produced during photoirradiation, and the faradic efficiency of HCOOH formation (=production selectivity) was $>80\%$, indicating that the hybrid photocatalyst InP/[MCE1+2-A] working as a photocathode selectively reduced CO_2 to formate photoelectrochemically in H_2O under simulated sunlight.

3.2. Solar-Driven Selective CO_2 Reduction to Formate with H_2O Oxidation Reaction by Tandem Configuration.

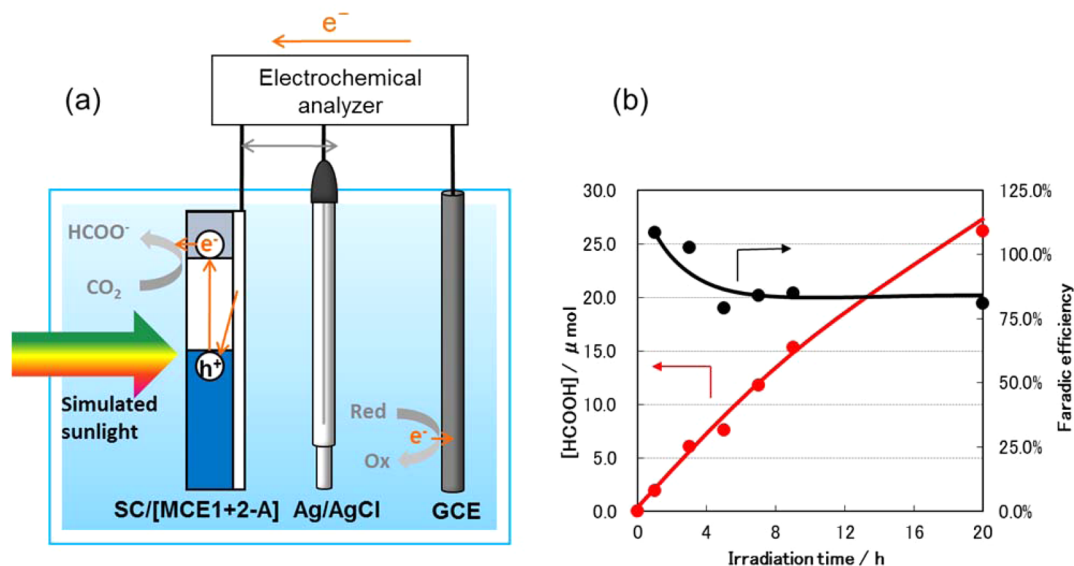


Figure 7. (a) Photoelectrochemical CO_2 reduction performed in pure H_2O using a three-electrode configuration. A photocathode (hybrid InP/[MCE1+2-A] photocatalyst), glassy carbon, and Ag/AgCl were used as the working, counter, and reference electrodes, respectively. (b) Photoelectrocatalytic $HCOOH$ formation from CO_2 as a function of the irradiation time over InP/[MCE1+2-A]. The applied potential was -0.4 V (vs Ag/AgCl), and irradiation was from simulated sunlight (1 SUN) under CO_2 . The graph shows the formation of $HCOOH$ (red line) and faradic efficiency (black line).

Some semiconductor photocatalysts possess a strong ability to photooxidize H_2O by extracting electrons, called the Z-scheme. For this system, two-step photoexcitation is conducted to allow conduction band electrons in the H_2O oxidation photocatalyst to compensate for holes in the photocathode in a photoexcited state. For example, heterogeneous semiconductors with different band-energy potentials for producing H_2 and O_2 from H_2O have been applied to systems for photocatalytic H_2O splitting.^{69–73} As a system for solar fuel production by CO_2 reduction in aqueous solution, a tandem configuration of photoanodes and photocathodes can be used to reproduce the Z-scheme. Because the InP/[MCE1+2-A] hybrid can reduce CO_2 to formate selectively in H_2O under visible-light irradiation, combining it with a semiconductor photocatalyst capable of H_2O oxidation should reproduce artificial photosynthesis, allowing solar-driven CO_2 reduction using H_2O as both an electron and a proton source through a Z-scheme system.

In photoelectrochemical reaction systems using electrode combinations, such as photocathodes and metal anodes, metal cathodes and photoanodes, or photocathodes and photoanodes, applying external electrical bias to assist the reactions is preferable. However, artificial photosynthesis should not require external electrical bias. To develop a system that selectively reduces CO_2 using H_2O as an electron donor with no external electrical bias, a Z-scheme system was developed (Figure 8) by functionally combining InP/[MCE1+2-A] with a photocatalyst for H_2O oxidation. The E_{VBM} value of the photocatalyst for H_2O oxidation must be more positive than the potential for H_2O oxidation (theoretically, 1.23 V vs NHE). Furthermore, the E_{CBM} value of the photocatalyst for H_2O oxidation should be more negative than that of the photocatalyst for CO_2 reduction. This will ensure electron transfer from the photocatalyst for H_2O oxidation to the photocatalyst for CO_2 reduction, with no external electrical bias. In this work, anatase titanium dioxide on a conducting glass (TiO_2) was used as the photocatalyst for H_2O oxidation, taking into account the

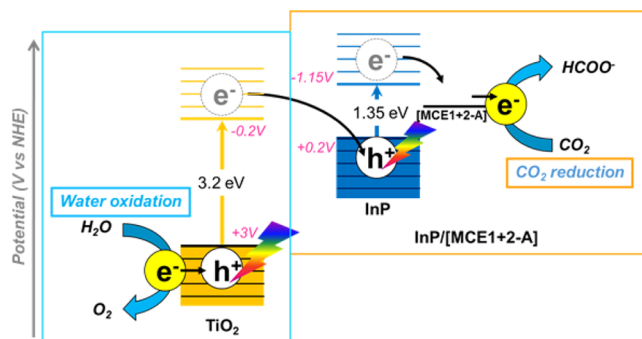


Figure 8. Schematic energy diagram of the total reaction of the Z-scheme system for CO_2 reduction. Adapted with permission from ref 92. Copyright 2011 American Chemical Society.

E_{CBM} value of TiO_2 , the E_{VBM} value of InP/[MCE1+2-A], and the O_2 generation ability of oxidizing H_2O .^{52–62} The potential difference between E_{CBM} of TiO_2 and E_{VBM} of InP (ΔE_{SS}) was estimated to be -0.4 V. Hence, successful electron transfer between two photocatalysts with no external electrical bias could be facilitated.⁹⁰ The reduction of CO_2 combined with H_2O oxidation was performed using a two-electrode configuration (Figure 9). The CO_2 reduction photocatalyst InP/[MCE1+2-A] (20×15 mm², colored black) and H_2O oxidation photocatalyst TiO_2 (20×15 mm², translucent) were used (TiO_2 //InP/[MCE1+2-A] system). A two-compartment Pyrex cell divided by a proton-exchange membrane was used as the reactor to prevent reoxidation of the formate over TiO_2 . Because the platinum (Pt) cocatalyst facilitates O_2 production from hydrogen peroxide (H_2O_2) originating from H_2O , the Pt cocatalyst was loaded onto the TiO_2 photocatalyst. A solution of 10 mM $NaHCO_3$, which also accelerated catalytic O_2 generation over the TiO_2 photocatalyst, was used as the electrolyte for InP/[MCE1+2-A].⁹¹ A solar simulator equipped with an air mass 1.5 filter (AM 1.5) was used as the light source with the intensity adjusted to 1 SUN. The irradiation area was

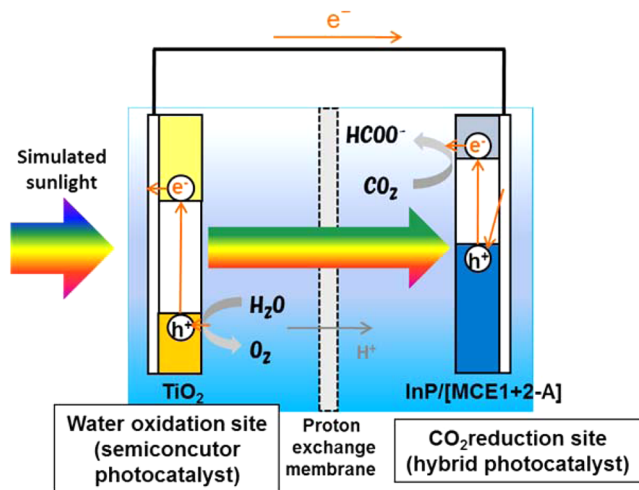


Figure 9. Schematic illustration of the tandem-cell reactor. Adapted with permission from ref 92. Copyright 2011 American Chemical Society.

$10 \times 10 \text{ mm}^2$. The TiO_2/Pt side was irradiated, while $\text{InP}/[\text{MCE1+2-A}]$ was irradiated with light transmitted through the TiO_2/Pt photocatalyst electrode and proton-exchange membrane. No external electrical bias was applied between the two photocatalysts. Stable photocatalytic production of formate was observed for 24 h under irradiation (1 SUN) with bubbled CO_2 (Figure 10).⁹² TN_{HCOOH} was >17 at 24 h; larger values would likely occur upon further irradiation. Even though H_2 and CO also were detected, faradic efficiency reached approximately 70%, a value similar to that observed over $\text{InP}/[\text{MCE1+2-A}]$ using a three-electrode configuration. The conversion efficiency from solar energy to chemical energy was ca. 0.04%, which was calculated by dividing the combustion heat of generated

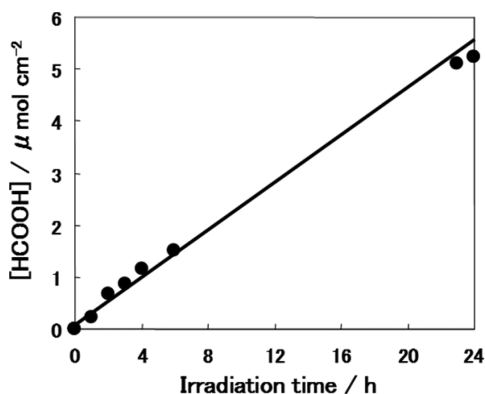
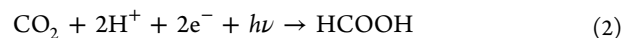
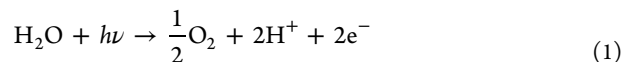


Figure 10. Photocatalytic HCOOH formation from CO_2 as a function of the irradiation time using a tandem configuration such as $\text{InP}/[\text{MCE1+2-A}]$ with TiO_2/Pt . CO_2 reduction was performed using a two-electrode configuration with no external electrical bias in 10 mM NaHCO_3 . $\text{InP}/[\text{MCE1+2-A}]$ and TiO_2/Pt were used as photocatalysts for CO_2 reduction and H_2O oxidation, respectively. A two-compartment Pyrex cell separated by a proton-exchange membrane (Nafion 117, DuPont) was used as the reactor. A solar simulator, in which the intensity was adjusted to 1 SUN (AM 1.5), was used as the light source. The TiO_2/Pt side was irradiated, while $\text{InP}/[\text{MCE1+2-A}]$ was irradiated with light transmitted through the translucent TiO_2/Pt and proton-exchange membrane. The irradiation area was $10 \times 10 \text{ mm}^2$. Adapted with permission from ref 92. Copyright 2011 American Chemical Society.

HCOOH by the integrated energy of the solar-simulating light (AM 1.5). This value was one-fifth (20%) of 0.2%, which is the solar conversion efficiency of switchgrass, a promising crop for biomass fuel.⁹³ Isotope tracer analysis using $^{13}\text{CO}_2$ and D_2O indicated that the carbon and proton sources of the formate were CO_2 and H_2O , respectively. A negligible amount of $\text{H}^{12}\text{COO}^-$ was observed for $^{13}\text{CO}_2$, even in the presence of $\text{H}^{12}\text{CO}_3^-$. These results indicate that the formate detected in the reaction was produced mainly from CO_2 molecules in solution, not from carbonate ions. Furthermore, gas chromatography–mass spectrometry (GC–MS) detected $^{18}\text{O}_2$ in the gas phase at the oxidation site after reaction using an aqueous solution containing 25% H_2^{18}O . These results confirmed that CO_2 was reduced to formate by electrons extracted from H_2O during the oxidation process to O_2 and that protons also originated from H_2O under simulated sunlight (eqs 1 and 2).



3.3. Improved Efficiency and Development of a Monolithic Device for CO_2 Reduction Using H_2O . Using a semiconductor/metal-complex hybrid photocatalyst, which supports solar formate production through the Z-scheme reaction utilizing only sunlight, CO_2 and H_2O were produced successfully without an external bias application. However, the conversion efficiency for solar energy to chemical energy (formate) was not adequate for the $\text{TiO}_2//\text{InP}/[\text{MCE1+2-A}]$ system.⁹⁴ Therefore, an improvement in the efficiency was needed to determine the feasibility of the artificial photosynthetic system. Because this concept can be applied to many inorganic semiconductors and metal-complex catalysts, the efficiency and reaction selectivity could be enhanced by optimizing the electron-transfer process by adjusting energy-band configurations, conjugation conformations, and catalyst structures. The photoinduced electron transfer from the semiconductor for H_2O oxidation to the semiconductor for CO_2 reduction was considered the rate-limiting step for selective CO_2 reduction in the $\text{TiO}_2//\text{InP}/[\text{MCE1+2-A}]$ system, and so we focused on this system. The energy difference ΔE_{SS} also was essential for improving the efficiency of the Z-scheme consisting of the semiconductor/metal-complex hybrid system (Figure 11).

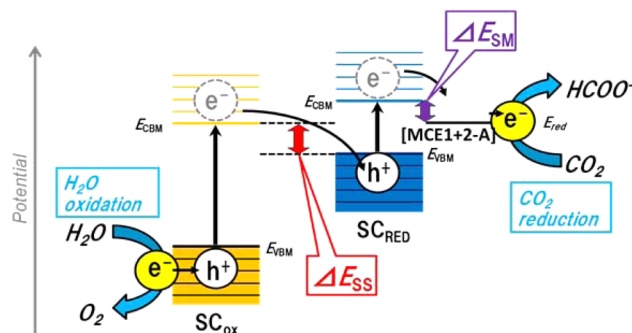


Figure 11. Total reaction of the Z-scheme system combining SC/ $[\text{MCE1+2-A}]$ photocatalyst for CO_2 reduction and SC_{OX} photocatalyst for H_2O oxidation. Adapted with permission from ref 94. Copyright 2013 Royal Society of Chemistry.

The next goal was to facilitate electron transfer from the E_{CBM} value of the photocatalyst for H_2O oxidation to the E_{VBM} value of the photocatalyst for CO_2 reduction. Using photo-induced C–V measurements, the onset potential of the TiO_2 photocatalyst was observed at -0.6 V (vs Ag/AgCl). To increase ΔE_{SS} , the E_{CBM} value of the photocathode must be more negative than that of TiO_2 . Therefore, TiO_2 was replaced with reduced SrTiO_3 (r-STO), which has a more negative onset potential of -0.75 V (vs Ag/AgCl). Thus, the r-STO//InP/[MCE1+2-A] system generated formate by reducing CO_2 using H_2O as an electron donor and a proton source. The conversion efficiency from solar energy to chemical energy reached 0.14%, which was 4-fold greater than that of the previous TiO_2 //InP/[MCE1+2-A] system⁹⁴ and was 70% of the solar conversion efficiency for switchgrass, a biomass crop. These results demonstrate that the band configuration of semiconductors is crucial for enhancing solar formate production from CO_2 and H_2O through the Z-scheme.

In general, semiconductor photocatalysts can oxidize organic compounds easily. For example, TiO_2 is a photocatalyst that photooxidizes various organic substances. Therefore, a proton-exchange membrane was necessary to prevent reoxidation of the reduction products, such as formate, over TiO_2 . However, r-STO has a unique catalytic ability for photooxidation, i.e., selective H_2O oxidation in the presence of formate (Figure 12).

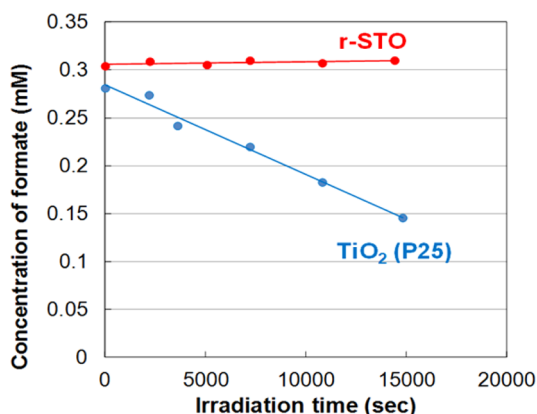


Figure 12. Comparison of photoelectrochemical degradation of HCOOH using r-STO and TiO_2 (P25). Adapted with permission from ref 94. Copyright 2013 Royal Society of Chemistry.

This feature of r-STO allows the construction of a simple system that does not require a proton-exchange membrane to avoid reoxidation of formate to CO_2 . On the basis of this selectivity over r-STO, an r-STO//InP/[MCE1+2-A] wireless monolithic device was fabricated and photoelectrochemical CO_2 reduction was conducted in a one-pot reactor, as shown in Figure 13. Formate ($0.88 \mu\text{mol}$) was produced over wireless r-STO/InP/[RuCP] during 3 h of irradiation using simulated sunlight (Table 1). The conversion efficiency from solar energy to chemical energy was ca. 0.08%. In contrast, a negligible amount of formate was detected over wireless TiO_2 //InP/[MCE1+2-A] in the one-pot reactor. This system is preferable to a wired conventional photoelectrochemical or electrochemical system because it does not contain wire connections or a proton-exchange membrane. This simple structure is practical, but its efficiency for solar-to-chemical energy conversion was not adequate and must be improved further.

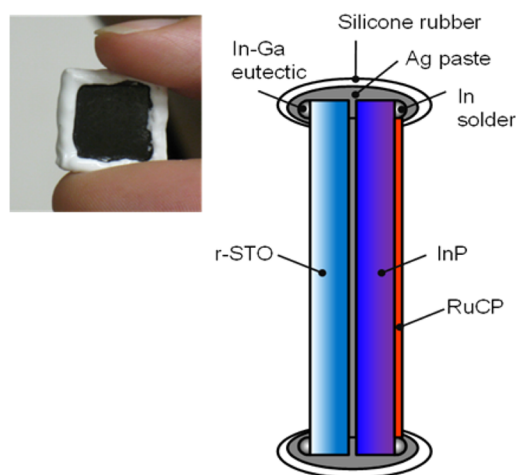


Figure 13. Schematic illustration of a single wireless cell of the r-STO/InP/[MCE1+2-A] hybrid catalyst. Adapted with permission from ref 94. Copyright 2013 Royal Society of Chemistry.

Table 1. Results of Photoelectrochemical CO_2 Reduction for Wired and Wireless Systems with No Electrical Bias^a

photocatalyst	connection	[HCOOH], μmol	solar conversion efficiency, %
TiO_2 //InP/[MCE1+2-A]	wired	0.33	0.03
r-STO//InP/[MCE1+2-A]	wired	1.45	0.14
TiO_2 /InP/[MCE1+2-A]	wireless	0	0.00
r-STO/InP/[MCE1+2-A]	wireless	0.94	0.08

^aThe light source was simulated sunlight, and the irradiation time was 3 h. Adapted with permission from ref 94. Copyright 2013 Royal Society of Chemistry.

4. CONCLUSIONS

The development of efficient artificial photosynthesis, a technology that mimics the photosynthesis of plants, has been pursued in an effort to achieve clean (“green”) energy. Direct conversion of solar energy to chemical energy through artificial photosynthesis could promote a carbon-neutral society. This report summarized recent research results on artificial photosynthetic systems operated under sunlight in which CO_2 reduction and H_2O oxidation were functionally conjugated within one system. Although many molecular photocatalysts for CO_2 reduction and H_2O oxidation have been developed, no reports of actual efficient solar conversion for CO_2 reduction reactions using H_2O as an electron donor under solar irradiation have been released. The different reaction conditions used for CO_2 reduction and H_2O oxidation make their conjugation a very difficult challenge.

The present study, which demonstrates artificial photosynthesis for the direct production of organic substances under sunlight using a hybrid photocatalyst composed of a semiconductor and a metal complex, shows promise for future progress in this field. This contribution to inorganic chemistry is significant not only for the development of inorganic photocatalysts for CO_2 reduction and H_2O oxidation but also for rapid progress in the development of semiconductor/metal-complex hybrid systems.

A recent report indicated that the combination of an external solar cell and a metal electrocatalyst used for CO_2 reduction could produce a solar conversion efficiency $>1\%$.⁹⁵ In contrast, a solar-to- H_2 conversion efficiency of over 10% has been

reported by combining a solar cell and a metal electrocatalyst for H₂ generation. However, an issue on the system cost still remains even in the field of solar H₂.⁹⁶ Thus, it is needless to say that more efficient and lower cost system is also required for CO₂ reduction. More effort is needed to develop an efficient photocatalyst within a simple and inexpensive artificial photosynthesis system.

■ ASSOCIATED CONTENT

■ Supporting Information

Materials, general procedures, and methods. This material is available free of charge via the Internet at <http://pubs.acs.org>.

■ AUTHOR INFORMATION

Corresponding Author

*E-mail: ssato@mosk.tytlabs.co.jp.

Notes

The authors declare no competing financial interest.

■ ACKNOWLEDGMENTS

The authors thank K. Uemura for experimental support.

■ REFERENCES

- (1) Ben-Shem, A.; Frolow, F.; Nelson, N. *Nature* **2003**, 426, 630.
- (2) Nelson, N.; Yocum, C. F. *Annu. Rev. Plant Biol.* **2006**, 57, 521.
- (3) Kanady, J. S.; Tsui, E. Y.; Day, M. W.; Agapie, T. *Science* **2011**, 333, 733.
- (4) Umena, Y.; Kawakami, K.; Shen, J.-R.; Kamiya, N. *Nature* **2011**, 473, 55.
- (5) Ahn, T. K.; Avenson, T. J.; Ballottari, M.; Cheng, Y.-C.; Niyogi, K. K.; Bassi, R.; Fleming, G. R. *Science* **2008**, 320, 794.
- (6) Hawecker, J.; Lehn, J.-M.; Ziessel, R. *Helv. Chim. Acta* **1986**, 69, 1990.
- (7) Hori, H.; Johnson, F. P. A.; Koike, K.; Ishitani, O.; Ibusuki, T. *J. Photochem. Photobiol. A: Chem.* **1996**, 96, 171.
- (8) Tsubaki, H.; Sekine, A.; Ohashi, Y.; Koike, K.; Takeda, H.; Ishitani, O. *J. Am. Chem. Soc.* **2005**, 127, 15544.
- (9) Kurz, P.; Probst, B.; Spingler, B.; Alberto, R. *Eur. J. Inorg. Chem.* **2006**, 15, 2966.
- (10) Bruckmeier, C.; Lehenmeier, N. W.; Reithmeier, R.; Rieger, B.; Herranz, J.; Kavakli, C. *Dalton Trans.* **2012**, 41, S026.
- (11) Chauvin, J.; Lafolet, F.; Chardon-Noblat, S.; Deronzier, A.; Jakonen, M.; Haukka, M. *Chem.—Eur. J.* **2011**, 17, 4313.
- (12) Sato, S.; Morikawa, T.; Kajino, T.; Ishitani, O. *Angew. Chem., Int. Ed.* **2013**, 52, 988.
- (13) Li, L.; Zhang, S.; Xu, L.; Wang, J.; Shi, L.-X.; Chen, Z.-N.; Hong, M.; Luo, J. *Chem. Sci.* **2014**, 5, 3808.
- (14) Kutal, C.; Weber, M. A.; Ferraudi, G.; Geiger, D. *Organometallics* **1985**, 4, 2161.
- (15) Kutal, C.; Corbin, A. J.; Ferraudi, G. *Organometallics* **1987**, 6, 553.
- (16) Hayashi, Y.; Kita, S.; Brunschwig, B. S.; Fujita, E. *J. Am. Chem. Soc.* **2003**, 125, 11976.
- (17) Takeda, H.; Koike, K.; Inoue, H.; Ishitani, O. *J. Am. Chem. Soc.* **2008**, 130, 2023.
- (18) Morris, A. J.; Meyer, G. J.; Fujita, E. *Acc. Chem. Res.* **2009**, 42, 1983.
- (19) Agarwal, J.; Fujita, E.; Schaefer, H. F., III; Muckerman, J. T. *J. Am. Chem. Soc.* **2012**, 134, 5180.
- (20) Kou, Y.; Nabetani, Y.; Masui, D.; Shimada, T.; Takagi, S.; Tachibana, H.; Inoue, H. *J. Am. Chem. Soc.* **2014**, 136, 6021.
- (21) Ogata, T.; Yanagida, S.; Brunschwig, B. S.; Fujita, E. *J. Am. Chem. Soc.* **1995**, 117, 6708.
- (22) Ooyama, D.; Tomon, T.; Tsuge, K.; Tanaka, K. *J. Organomet. Chem.* **2001**, 619, 299.
- (23) Kimura, E.; Bu, X.; Shionoya, M.; Wada, S.; Maruyama, S. *Inorg. Chem.* **1992**, 31, 4542.
- (24) Kimura, E.; Haruta, M.; Koike, T.; Shionoya, M.; Takenouchi, K.; Iitaka, Y. *Inorg. Chem.* **1993**, 32, 2779.
- (25) Mochizuki, K.; Manaka, S.; Takeda, I.; Kondo, T. *Inorg. Chem.* **1996**, 35, 5132.
- (26) Komatsuzaki, N.; Himeda, Y.; Takeuji, H.; Sugihara, H.; Kasuga, K. *Bull. Chem. Soc. Jpn.* **1999**, 72, 725.
- (27) Gholamkhass, B.; Mametsuka, H.; Koike, K.; Tanabe, T.; Furue, M.; Ishitani, O. *Inorg. Chem.* **2005**, 44, 2326.
- (28) Morimoto, T.; Nishiura, C.; Tanaka, M.; Rohacova, J.; Nakagawa, Y.; Funada, Y.; Koike, K.; Yamamoto, Y.; Shishido, S.; Kojima, T.; Saeki, T.; Ozeki, T.; Ishitani, O. *J. Am. Chem. Soc.* **2013**, 135, 13266.
- (29) Tamaki, Y.; Morimoto, T.; Koike, K.; Ishitani, O. *Proc. Natl. Acad. Sci. U.S.A.* **2012**, 109, 15673.
- (30) Tamaki, Y.; Koike, K.; Morimoto, T.; Yamazaki, Y.; Ishitani, O. *Inorg. Chem.* **2013**, 52, 11902.
- (31) Kuramochi, Y.; Kamiya, M.; Ishida, H. *Inorg. Chem.* **2014**, 53, 3326.
- (32) Takeda, H.; Koizumi, H.; Okamoto, K.; Ishitani, O. *Chem. Commun.* **2014**, 50, 1491.
- (33) Huang, Z.; Luo, Z.; Geletii, Y. V.; Vickers, J.; Yin, Q.; Wu, D.; Hou, Y.; Ding, Y.; Song, J.; Musaev, D. G.; Hill, C. L.; Lian, T. *J. Am. Chem. Soc.* **2011**, 133, 2068.
- (34) Roeser, S.; Fàrrs, P.; Bozoglian, F.; Martínez-Belmonte, M.; Benet-Buchholz, J.; Llobet, A. *ChemSusChem* **2011**, 4, 197.
- (35) McDaniel, N. D.; Coughlin, F. J.; Tinker, L. L.; Bernhard, S. *J. Am. Chem. Soc.* **2008**, 130, 210.
- (36) Geletii, Y. V.; Huang, Z.; Hou, Y.; Musaev, D. G.; Lian, T.; Hill, C. L. *J. Am. Chem. Soc.* **2009**, 131, 7522.
- (37) Han, X.-B.; Zhang, Z.-M.; Zhang, T.; Li, Y.-G.; Lin, W.; You, W.; Su, Z.-M.; Wang, E.-B. *J. Am. Chem. Soc.* **2014**, 136, 5359.
- (38) Shevchenko, D.; Anderlund, M. F.; Thapper, A.; Styring, S. *Energy Environ. Sci.* **2011**, 4, 1284.
- (39) Song, F.; Ding, Y.; Ma, B.; Wang, C.; Wang, Q.; Du, X.; Fu, S.; Song, J. *Energy Environ. Sci.* **2013**, 6, 1170.
- (40) Tanaka, S.; Annaka, M.; Sakai, K. *Chem. Commun.* **2012**, 48, 1653.
- (41) Lv, H.; Song, J.; Geletii, Y. V.; Vickers, J. W.; Sumliner, J. M.; Musaev, D. G.; Kögerler, P.; Zhuk, P. F.; Bacsá, J.; Zhu, G.; Hill, C. L. *J. Am. Chem. Soc.* **2014**, 136, 9268.
- (42) Halmann, M. *Nature* **1978**, 275, 115.
- (43) Inoue, T.; Fujishima, A.; Konishi, S.; Honda, K. *Nature* **1979**, 277, 637.
- (44) Sayama, K.; Arakawa, H. *J. Phys. Chem.* **1993**, 97, 531.
- (45) Krejčíková, S.; Matějová, L.; Kočí, K.; Obalová, L.; Matěj, Z.; Čapek, L.; Šolcová, O. *Appl. Catal., B* **2012**, 111.
- (46) Pan, J.; Wu, X.; Wang, L.; Liu, G.; Lu, G. Q.; Cheng, H. M. *Chem. Commun.* **2011**, 47, 8361.
- (47) Iizuka, K.; Wato, T.; Miseki, Y.; Saito, K.; Kudo, A. *J. Am. Chem. Soc.* **2011**, 133, 20863.
- (48) Fujiwara, H.; Hosokawa, H.; Murakoshi, K.; Wada, Y.; Yanagida, S.; Okada, T.; Kobayashi, H. *J. Phys. Chem. B* **1997**, 101, 8270.
- (49) Kanemoto, M.; Shiragami, T.; Pac, C.; Yanagida, S. *J. Phys. Chem.* **1992**, 96, 3521.
- (50) Inoue, H.; Moriwaki, H.; Maeda, K.; Yoneyama, H. *J. Photochem. Photobiol., A* **1995**, 86, 191.
- (51) Teramura, K.; Iguchi, S.; Mizuno, Y.; Shishido, T.; Tanaka, T. *Angew. Chem., Int. Ed.* **2012**, 51, 8008.
- (52) Fujishima, A.; Honda, K. *Nature* **1972**, 238, 37.
- (53) Sato, S.; White, J. M. *Chem. Phys. Lett.* **1980**, 72, 83.
- (54) Kudo, A.; Omori, K.; Kato, H. *J. Am. Chem. Soc.* **1999**, 121, 11459.
- (55) Hara, M.; Hitoki, G.; Takata, T.; Kondo, J. N.; Kobayashi, H.; Domen, K. *Catal. Today* **2003**, 78, 555.
- (56) Hitoki, G.; Takata, T.; Kondo, J. N.; Hara, M.; Kobayashi, H.; Domen, K. *Chem. Commun.* **2002**, 16, 1698.

- (57) Santato, C.; Ulmann, M.; Augustynski, J. *J. Phys. Chem. B* **2001**, *105*, 936.
- (58) Kay, A.; Cesar, I.; Gratzel, M. *J. Am. Chem. Soc.* **2006**, *128*, 15714.
- (59) Sayama, K.; Nomura, A.; Arai, T.; Sugita, T.; Abe, R.; Yanagida, M.; Oi, T.; Iwasaki, Y.; Abe, Y.; Sugihara, H. *J. Phys. Chem. B* **2006**, *110*, 11352.
- (60) Kudo, A.; Miseki, Y. *Chem. Soc. Rev.* **2009**, *38*, 253.
- (61) Abe, R.; Higashi, M.; Domen, K. *J. Am. Chem. Soc.* **2010**, *132*, 11828.
- (62) Higashi, M.; Domen, K.; Abe, R. *J. Am. Chem. Soc.* **2013**, *135*, 10238.
- (63) Yang, C.-C.; Yu, Y.-H.; van der Linden, B.; Wu, J. C. S.; Mul, G. *J. Am. Chem. Soc.* **2010**, *132*, 8398.
- (64) Yui, T.; Kan, A.; Saitoh, C.; Koike, K.; Ibusuki, T.; Ishitani, O. *ACS Appl. Mater. Interfaces* **2011**, *3*, 2594.
- (65) Nozik, A. J. *Appl. Phys. Lett.* **1977**, *30*, 567.
- (66) Dominey, R. N.; Lewis, N. S.; Bruce, J. A.; Bookbinder, D. C.; Wrighton, M. S. *J. Am. Chem. Soc.* **1982**, *104*, 467.
- (67) Khaselev, O.; Turner, J. A. *Science* **1998**, *280*, 425.
- (68) Maeda, K.; Teramura, K.; Liu, D.; Takata, T.; Saito, N.; Inoue, Y.; Domen, K. *Nature* **2006**, *440*, 295.
- (69) Leygraf, C.; Hendewerk, M.; Somorjai, G. A. *J. Phys. Chem.* **1982**, *86*, 4484.
- (70) Sayama, K.; Mukasa, K.; Abe, R.; Abe, Y.; Arakawa, H. *Chem. Commun.* **2001**, *35*, 2416.
- (71) Sasaki, Y.; Nemoto, H.; Saito, K.; Kudo, A. *J. Phys. Chem. C* **2009**, *113*, 17536.
- (72) Ma, S. S. K.; Maeda, K.; Hisatomi, T.; Tabata, M.; Kudo, A.; Domen, K. *Chem.—Eur. J.* **2013**, *19*, 7480.
- (73) Iwase, A.; Ng, Y. H.; Ishiguro, Y.; Kudo, A.; Amal, R. *J. Am. Chem. Soc.* **2011**, *133*, 11054.
- (74) Sato, S.; Morikawa, T.; Saeki, S.; Kajino, T.; Motohiro, T. *Angew. Chem., Int. Ed.* **2010**, *49*, 5101.
- (75) Ishida, H.; Terada, T.; Tanaka, K.; Tanaka, T. *Organometallics* **1987**, *6*, 181.
- (76) Tanaka, K. *Bull. Chem. Soc. Jpn.* **1998**, *71*, 17.
- (77) Yamanaka, K.; Sato, S.; Iwaki, M.; Kajino, T.; Morikawa, T. *J. Phys. Chem. C* **2011**, *115*, 18348.
- (78) Morikawa, T.; Saeki, S.; Suzuki, T.; Kajino, T.; Motohiro, T. *Appl. Phys. Lett.* **2010**, *96*, 142111.
- (79) Asahi, R.; Morikawa, T.; Ohwaki, T.; Aoki, K.; Taga, Y. *Science* **2001**, *293*, 269.
- (80) Nakano, Y.; Morikawa, T.; Ohwaki, T.; Taga, Y. *Appl. Phys. Lett.* **2006**, *88*, 172103.
- (81) Suzuki, T. M.; Tanaka, H.; Morikawa, T.; Iwaki, M.; Sato, S.; Saeki, S.; Inoue, M.; Kajino, T.; Motohiro, T. *Chem. Commun.* **2011**, *47*, 8673.
- (82) Kumar, B.; Smieja, J. M.; Kubiak, C. P. *J. Phys. Chem. C* **2010**, *114*, 14220.
- (83) Arai, T.; Sato, S.; Uemura, K.; Morikawa, T.; Kajino, T.; Motohiro, T. *Chem. Commun.* **2010**, *46*, 6944.
- (84) Arai, T.; Tajima, S.; Sato, S.; Uemura, K.; Morikawa, T.; Kajino, T. *Chem. Commun.* **2011**, *47*, 12664.
- (85) Sekizawa, K.; Maeda, K.; Koike, K.; Domen, K.; Ishitani, O. *J. Am. Chem. Soc.* **2013**, *135*, 4596.
- (86) Maeda, K.; Sekizawa, K.; Ishitani, O. *Chem. Commun.* **2013**, *49*, 10127.
- (87) Chardon-Noblat, S.; Deronzier, A.; Ziessel, R.; Zsoldos, D. *J. Electrochem. Soc.* **1998**, *444*, 253.
- (88) Huang, J.; Stockwell, D.; Huang, Z.; Mohler, D. L.; Lian, T. *J. Am. Chem. Soc.* **2008**, *130*, 5632.
- (89) Guzelian, A. A.; Katari, J. E. B.; Kadavanich, A. V.; Banin, U.; Hamad, K.; Juban, E.; Alivisatos, A. P. *J. Phys. Chem.* **1996**, *100*, 7212.
- (90) Ida, S.; Yamada, K.; Matsunaga, T.; Hagiwara, H.; Matsumoto, Y.; Ishihara, T. *J. Am. Chem. Soc.* **2010**, *132*, 17343.
- (91) Sayama, K.; Augustynski, J.; Arakawa, H. *Chem. Lett.* **2002**, 994.
- (92) Sato, S.; Arai, T.; Morikawa, T.; Uemura, K.; Suzuki, T. M.; Tanaka, H.; Kajino, T. *J. Am. Chem. Soc.* **2011**, *133*, 15240.
- (93) Lewandowski, I.; Scurlock, J. M. O.; Lindvall, E.; Christou, M. *Biomass Bioenergy* **2003**, *25*, 335.
- (94) Arai, T.; Sato, S.; Kajino, T.; Morikawa, T. *Energy Environ. Sci.* **2013**, *6*, 1274.
- (95) White, J. L.; Herb, J. T.; Kaczur, J. J.; Majsztrik, P. W.; Bocarsly, A. B. *J. CO₂ Util.* **2014**, *7*, 1.
- (96) Pinaud, B. A.; Benck, J. D.; Seitz, L. C.; Forman, A. J.; Chen, Z.; Deutsch, T. G.; James, B. D.; Baum, K. N.; Baum, G. N.; Ardo, S.; Wang, H.; Miller, E.; Jaramillo, T. F. *Energy Environ. Sci.* **2013**, *6*, 1983.